# ESR study of the frustrated $S = \frac{1}{2}$ chain magnet $LiCuVO_4$ in spiral and spin-modulated phases

L. A. Prozorova,[1] L. E. Svistov,[1,*] A. M. Vasiliev,[1] and A. Prokofiev[2]
[1]*P.L. Kapitza Institute for Physical Problems RAS, 119334 Moscow, Russia*
[2]*Institut für Festkörperphysik Technische Universität Wien, A-1040 Wien, Austria*
(Received 28 March 2016; revised manuscript received 9 September 2016; published 2 December 2016)

We report on the electron spin resonance (ESR) study of $LiCuVO_4$ in spiral and spin-modulated phases ($0 < \mu_0 H < 10$ T). The measurements have been made on high quality samples that allowed getting rid of absorption lines arising from defects. In the field range of spiral phase ($0 < \mu_0 H < 7.5$ T) all observed branches of the spectrum can be ascribed to uniform oscillations of planar spin structure. The ESR spectrum observed in spin-modulated phase ($\mu_0 H > 7.5$ T) has two branches. One of them can be explained by uniform oscillations of spin structure, whereas the second branch, surprisingly demonstrates only a weak dependence on field orientation, which indicates the exchange nature of this mode. Allegedly this mode can be associated with soliton excitations.

DOI: 10.1103/PhysRevB.94.224402

## I. INTRODUCTION

Quantum-spin chains with frustrated exchange interactions were among the most interesting issues for both experimental and theoretical research in condensed matter physics in the past decade [1–3]. The enhanced effect of quantum fluctuations imposed upon a fine balance of exchange interactions leads to a variety of novel ground states and phase transformations in these systems [4–7]. $LiCuVO_4$ is an example of a quasi-one-dimensional (quasi-1D) magnet with a competition of ferromagnetic and antiferromagnetic exchange interactions between nearest-neighbor ($J_1$) and next-nearest-neighbor ($J_2$) in-chain magnetic moments. A helical incommensurate structure is stabilized in this system below $T_N \approx 2.3$ K as a result of this particular combination of exchange interactions [8]. A strong reduction of the ordered spin component of $Cu^{2+}$ ions in this state $\langle\mu\rangle/\mu_B \simeq 0.3$ (Refs. [8,9]) provides evidence that the system partially retains properties of 1D chains.

Moderate applied magnetic fields 7–8 T induce a transformation of the spin helix into a collinear spin-modulated (SM) structure when all spins are parallel to the field, with their ordered components modulated along the chain with an incommensurate period [10,11]. This transition may be related to the field evolution of short-range chiral (transverse) and spin-density wave (longitudinal) correlations for the 1D $J_1$-$J_2$ model [12].

In the field range just below the saturation field the theory predicts the presence of a long-range nematic ordering [7,13]. The magnetic properties of $LiCuVO_4$ in this field range were studied by nuclear magnetic resonance (NMR) and pulse magnetization techniques [14,15]. These experiments have specified the supposed field range where the spin nematic phase can exist. The experiments discussed in our report were performed at fields far below this range. This work is focused on the magnetic properties of $LiCuVO_4$ in the helical and the SM phases at lowest temperatures and the spin-liquid phase at elevated temperatures.

*svistov@kapitza.ras.ru

## II. EXPERIMENTAL RESULTS

Single crystals of $LiCuVO_4$ grown by the method described in Ref. [16] belong to the same series as the samples studied in our previous high field NMR and calorimetric experiments [15,17]. Electron spin resonance (ESR) experiments were performed with a transmission-type spectrometer using different microwave modes of volume resonators in the frequency range $17 < \nu < 110$ GHz. The magnetic field of a superconducting solenoid was varied in the range $0 < \mu_0 H < 10$ T. The temperature was varied within the range $1.3 < T < 4.2$ K.

Figures 1 and 2 show the frequency-field diagrams of the ESR measured at $H \parallel \mathbf{a},\mathbf{b}$ and $H \parallel \mathbf{c}$, respectively. The spectra were obtained in the magnetically ordered phase at $T = 1.3$ K. Examples of the observed ESR spectra are shown in Figs. 3 and 4. The resonance absorption lines corresponding to different branches are marked by I–V. The branches I and II correspond to the low field range below the spin-flop reorientation $H_{sf} = 2.5$ T for the field directed parallel to $ab$ plane of the crystal. At these fields the static field lies in the spin plane. Branches III and IV are observed at $H_{sf} < H < H_c$, where $H_c = 6.9$ T for the fields $H \parallel \mathbf{a},\mathbf{b}$ and at $H < H_c$, where $H_c = 6.4$ T for the field $H \parallel \mathbf{c}$. These branches correspond to the field ranges where static field is perpendicular to the spin plane. The field $H_c$ given on Figs. 1– 4 with the dashed line marks the field where the spectra drastically changes. The values of $H_c$ are close to values of transition fields from the spiral phase to the spin-modulated phase obtained from magnetization experiments: $7.6 \pm 0.2$ T at $H \parallel \mathbf{a},\mathbf{b}$ and $6.7 \pm 0.2$ T at $H \parallel \mathbf{c}$ [14].

The resonance absorption lines corresponding to branches I–IV are in consent with more intensive ESR resonance lines observed in the samples used in Refs. [10,18]. Weak absorption lines, reported in these works, are not detected in our experiments performed on the samples with controlled quality.

The solid lines I, II and III, IV present the theoretical computation of the ESR spectrum for a planar spiral structure with uniaxial anisotropy below and above spin-flop reorientation [10]. The computations were done for a model of exchange-rigid planar spin structure [19] characterized by two susceptibilities $\chi_\parallel$ and $\chi_\perp$ for the static field directed parallel and perpendicular to a normal $\mathbf{n}$ to the spin plane

 

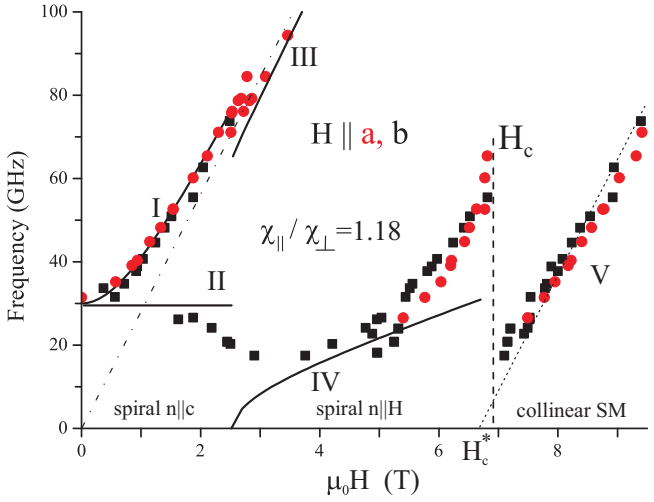


FIG. 1. The frequency-field diagram of ESR measured at $H \parallel \mathbf{a}$ (red circles) and $H \parallel \mathbf{b}$ (black squares) at $T = 1.3$ K. The dashed line marks the field boundary between the spiral and SM phases. The solid lines I, III and II, IV show computed branches of the ESR for planar spiral structure before and after spin-flop reorientation. The dash-dotted line shows the ESR mode in the paramagnetic state ($T = 4.2$ K) with $g_{a,b} = 2.08$. The dotted line is the fitting result of branch V with dependency: $\nu = (g_{ab}\mu_B/h)(H - H_c^*)$.

[10]. The anisotropic contribution to the magnetic energy, within the model, was taken into consideration with the term: $U_a = Dn_z^2$ ($D < 0$). The solid curves are computed with the following fitting parameters: $\chi_\parallel/\chi_\perp = 1.18$ and frequency gap of 30 GHz determined by uniaxial anisotropy. With the field approaching $H_c$ the intensity of the mode IV decreases and the field dependence of the resonance frequency deviates increasingly from the theoretical calculations. This deviation

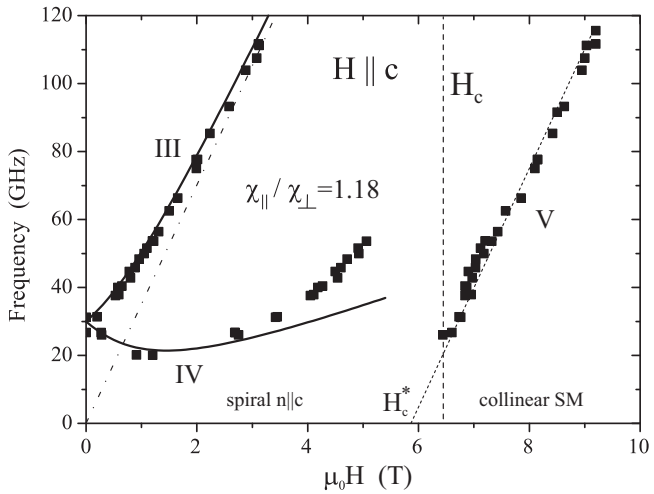


FIG. 2. The frequency-field diagram of the ESR measured at $H \parallel \mathbf{c}$ at $T = 1.3$ K. The dashed line marks the field boundary between the spiral and SM phases. The solid lines III and IV show computed branches of the ESR for planar spiral structure. The dash-dotted line shows the ESR mode in the paramagnetic state ($T = 4.2$ K) with $g_c = 2.46$. The dotted line is the fitting result of branch V with dependency: $\nu = (g_c\mu_B/h)(H - H_c^*)$.

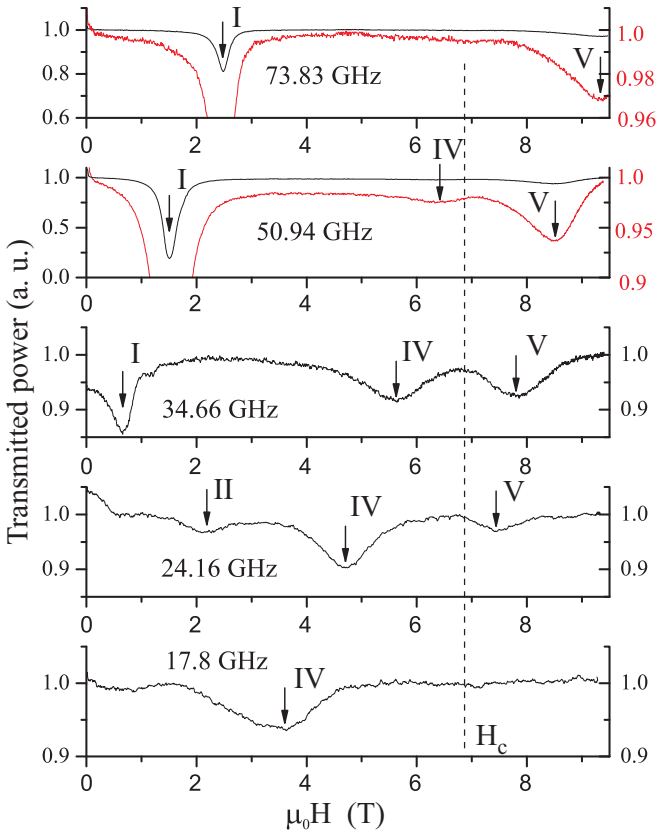


FIG. 3. The examples of ESR lines measured at $H \parallel \mathbf{b}$ and $T = 1.3$ K. The absorption lines are marked with symbols I–V in accordance with the designation of Figs. 1 and 2. Red lines represent the same spectra given in the expanded scale shown to the right.

can be qualitatively explained by an increase of anisotropy of exchange susceptibility $\chi_\parallel/\chi_\perp$ from 1.18 to 1.3 in the vicinity of transition. The dash-dotted lines in Figs. 1 and 2 present field dependencies of the ESR frequency in paramagnetic state with $g_{a,b} = 2.08$ and $g_c = 2.46$ at $T = 4.2$ K. These values of $g$ factors are close to the values obtained in old samples [20].

Two excitation modes were observed in the fields above $H_c$: the quasiparamagnetic branch, III, and the low frequency branch, V. According to Refs. [10,18] the quasiparamagnetic branch does not demonstrate any singularity at the transition field $H_c$, and also does not show detectable shift at the temperature of transition to the magneto-ordered state. The low frequency branch V starts at the transition field $H_c$ from the frequency $\approx$20 GHz and demonstrates monotonic growth with the field.

The temperature evolution of the ESR absorption lines at $H \parallel \mathbf{a}$ and excitation frequency $\nu = 26.2$ GHz is shown in Fig. 5. The transmitted power $P_{\rm tr}$ is normalized to a unity level at high fields ($\mu_0 H \approx 9$ T) for all records. $P_{\rm tr}(H)$ measured at temperatures smaller than 2.9 K are shifted along the $y$ axis for clear representation. The spectra shown with colored dotted lines represent the same spectra given in the expanded scale shown to the right. The absorption line V shifts to smaller fields and broadens with increasing temperature. The small absorption corresponding to this mode was observed even at temperature $T = 2.9$ K, which is higher than Néel

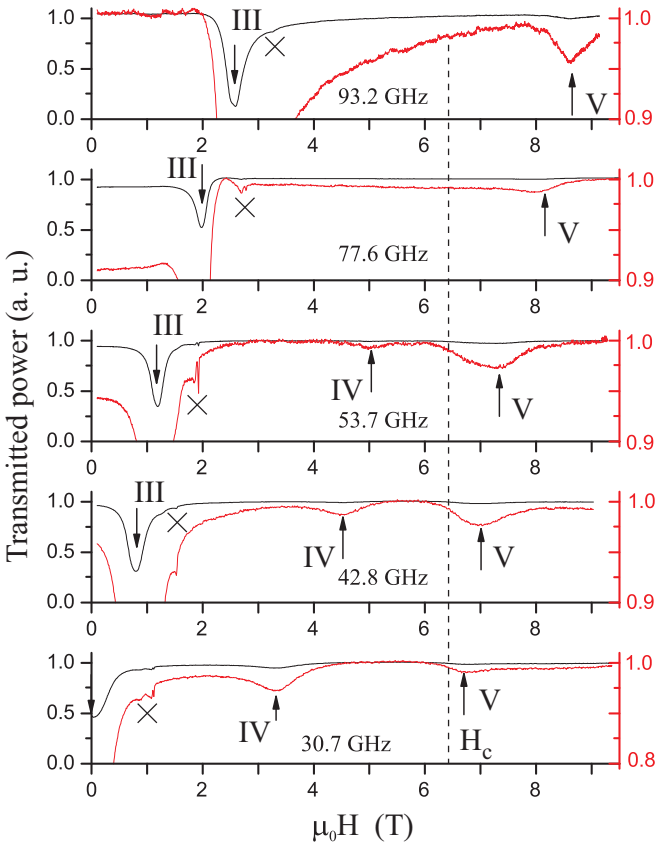


FIG. 4. Examples of ESR lines measured at $H \parallel \mathbf{c}$ and $T = 1.3$ K. The absorption lines are marked with symbols III, IV, and V in accordance with the designation of Figs. 1 and 2. Crosses mark weak paramagnetic absorption lines from Diphenylpicrylhydrazyl (DPPH) used for field calibration and cavity background. Red lines represent the same spectra given in the expanded scale shown to the right.

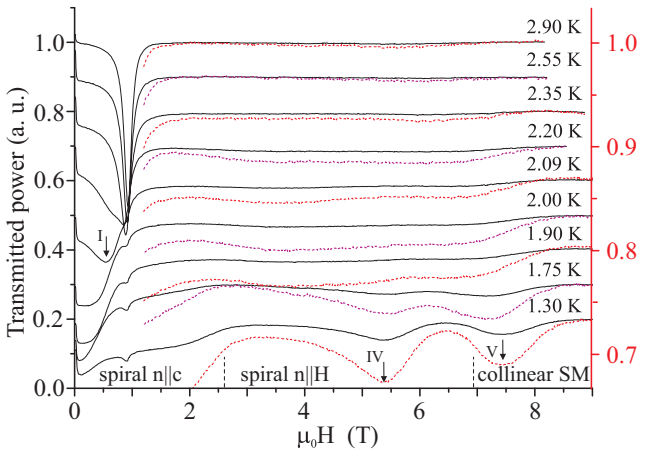


FIG. 5. The temperature evolution of ESR lines measured at $H \parallel \mathbf{a}$ and at excitation frequency: $\nu = 26.2$ GHz. Colored dotted lines represent the same spectra given in the expanded scale shown to the right. The absorption lines are marked with symbols I, IV, and V in accordance with the designation of Figs. 1 and 2. Dashed lines mark the field boundaries between magnetic phases at $T = 1.3$ K.

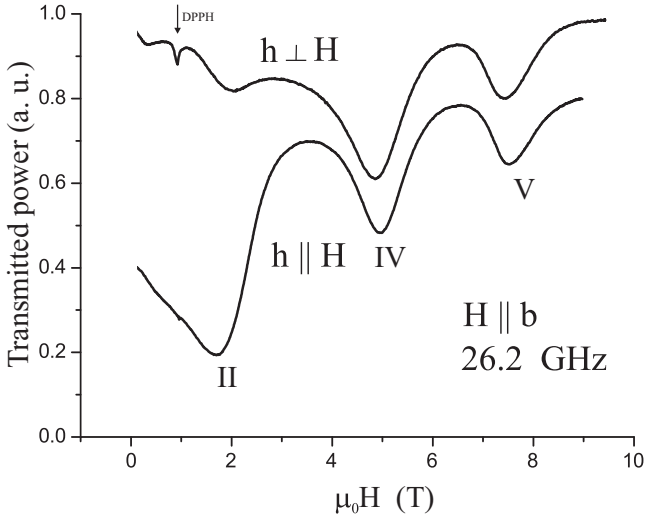


FIG. 6. Examples of the ESR lines measured at $H \parallel \mathbf{b}$ and $T = 1.3$ K and different polarization conditions: $h \parallel H$ and $h \perp H$. The absorption lines are marked with symbols in accordance with the designation of Figs. 1 and 2.

temperature $T_N \approx 2.3$ K. The Néel temperature is marked by the shift of the absorption line I from the field of the electron paramagnetic resonance.

Figure 6 demonstrates ESR absorption lines measured at $H \parallel b$, $T = 1.3$ K and different polarizations of microwave field **h** parallel and perpendicular to external field. The sample was placed in corresponding places within the resonator to provide these polarizations experimentally. The absorption line II is very sensitive to polarization of high frequency field. According to the model of spiral spin structure situated within the $ab$ plane the branch II corresponds to oscillations of the spin plane around the field direction [19]. As a result the excitation of this branch must be effective at $h \parallel H$, which agrees with the observation. The branches IV and V can be successively excited by both polarizations.

Figure 7 shows the temperature evolution of ESR absorption lines at $H \parallel \mathbf{c}$ and $\nu = 53.1$ GHz. A transmitted power $P_{\text{tr}}$ is normalized to a unit level at high fields ($\mu_0 H > 2$ T) for all records. $P_{\text{tr}}(H)$ measured at temperatures higher than 1.3 K are shifted along the $y$ axis for better representation. The absorption at all temperatures can be considered as a combination of a Lorentz line and a field independent absorption at fields below resonance. The red lines in Fig. 7 demonstrate the fitting result of experimental spectra by the following expression:

$$P_{\text{tr}} = 1 - \frac{A}{1 + [(H - H_R)/\Delta H]^2} - \frac{a}{1 + e^{(H - H_R)/\Delta h}}.$$

The second term of the expression describes the Lorentz line at the resonance field $H_R$. The third term phenomenologically approximates the low field nonresonance absorption by Fermi-like step function. Amplitudes $A$, $a$ and line widths $\Delta H$ and $\Delta h$ are shown in Fig. 8 where both absorption parts are given separately for the ESR line measured at $T = 2.42$ K and $\nu = 53.1$ GHz. As shown in Fig. 7 the $H_R$ shifts from the resonance field in the paramagnetic state $H_R = \nu/(g_c \mu_B/h)$

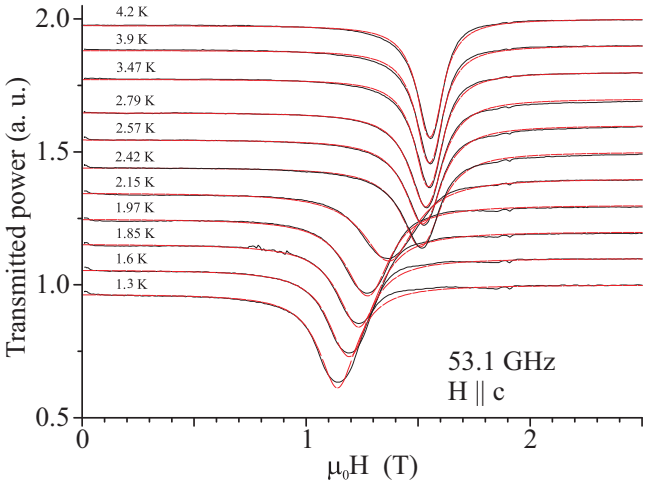


FIG. 7. Black lines show the temperature evolution of the ESR lines at $H \parallel \mathbf{c}$ and $\nu = 53.1$ GHz. All lines are normalized to 1 for high fields (see spectrum measured at $T = 1.3$ K). The spectra measured at higher temperatures are shifted along the $y$ axis for better representation. Red lines demonstrate the results of fitting by combination of the Lorentz single line and steplike Fermi function.

($g_c = 2.46$ at $T = 4.2$ K) to the lower fields in the magnetically ordered state. The temperature dependence of $H_R$ shown in Fig. 9 with black squares can be well described by the temperature dependence of the ESR energy gap [10]. The integral intensity of the Lorentz contribution to the absorption does not show noticeable singularity at the ordering, whereas the linewidth $\Delta H$ (free squares on Fig. 9) of this line exhibits sharp anomaly at $T_N \approx 2.3$ K. The integral intensity of the nonresonance part of absorption, which can be found as $a * H_R$, attains the maximum near the ordering temperature. The nonresonance absorption was also observed at other frequencies.

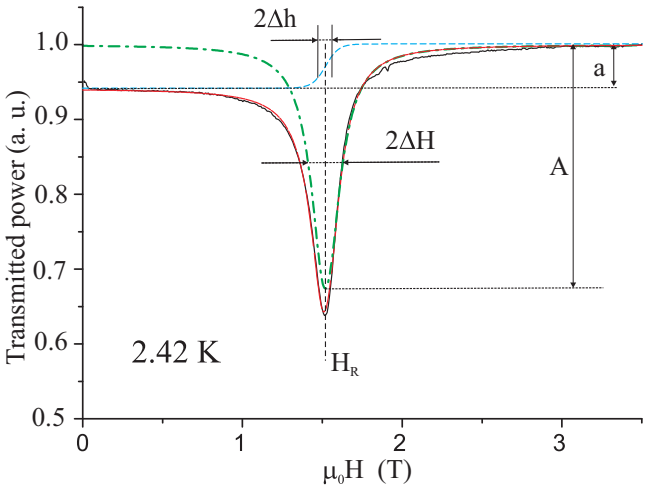


FIG. 8. The black line shows the ESR line measured at $H \parallel \mathbf{c}$, $T = 2.42$ K and $\nu = 53.1$ GHz. The red line shows the result of fitting with sum of Lorentz line (green dash-dotted line) and steplike Fermi function (blue dashed line).

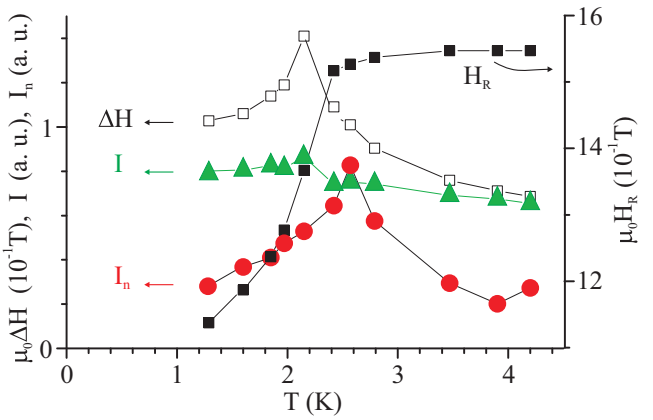


FIG. 9. Temperature dependencies of resonance field $H_R$ (black squares), linewidth $\Delta H$ (open squares), and integral intensity $I$ (green triangles) of the Lorentz-like part of the absorption and integral intensity of nonresonance steplike absorption $I_n$ (red circles).

## III. DISCUSSION

An ESR study of high quality $LiCuVO_4$ crystals demonstrates that the number of absorption lines observed in the experiments with new samples was significantly reduced compared to previous observations. The resonances observed in the present work are in good agreement with more intensive absorption lines observed on the samples from previous batches [10,18]. Thus, we believe that the observed branches are inherent to intrinsic magnetic excitation modes of $LiCuVO_4$.

All branches of the spectrum in the field range of the spiral phase ($0 < \mu_0 H < \mu_0 H_c$) can be ascribed to uniform oscillations of the planar spin structure. The theoretical dependencies are given with solid lines.

The nonresonance absorption is observed in the field range, where the three-dimensional (3D) spiral magnetic order at low temperature takes place, i.e., $H < H_c$, and at the fields below the field of uniform resonance $H_R$ (see Figs. 7–9). It is natural to attribute the observed nonresonance absorption to the excitation of magnons with nonzero wave vectors, which have frequencies larger than the frequency of the uniform mode and must resonate at smaller fields [21,22]. It is necessary to assume a special excitation mechanism of nonuniform modes to explain the nonresonant absorption, since the wave vector of such excitations differs from the wave vector of the high frequency electromagnetic pump which is approximately zero. The nonmagnetic defects within magnetic $Cu^{2+}$ chains can be important for excitation of nonuniform modes, since such defects can provide the boundary conditions for efficient excitation of standing waves with the large wave vectors.

The presence of such defects was suggested for interpretation of results of the NMR and calorimetry study of $LiCuVO_4$ [15,17]. The quasi-one-dimensionality of the system is essential for excitation of the standing magnetic wave modes with boundaries at defects within individual chains. The nonresonant part of the absorption was observed in a broad range around the ordering temperature, which allegedly are explained by nonuniform excitations located at the defects. The presence of the short-range long-living magnetic correlations

was observed at the temperatures beyond $T_N$ by NMR study of magnetic structure [23]. A composition study of $LiCuVO_4$ reveals a Li deficiency in a few percent even in crystals grown by the low temperature technique which provides crystals of the highest quality. It was argued that the Li deficiency results in holes with spins $S = 1/2$ localized on oxygen which, in turn, form a Zhang-Rice singlet with the neighboring copper spin [16,24]. Such a singlet should be equivalent to a nonmagnetic impurity replacing a Cu spin and will provoke an unusual magnetic state in its vicinity with the two nearest ferromagnetic exchange bonds removed, but with a conserved antiferromagnetic bond between the two parts of the interrupted chain. The presence of such defects in $LiCuVO_4$ single crystals of the same growing technique as in this work was suggested in order to explain the bulk magnetization process, as well as the vanadium NMR spectra near the saturation field [15] and results of the specific heat study [17]. Thus the observation of nonresonance absorption demonstrates the presence of an effective mechanism of the excitation of nonuniform oscillations, but this mechanism is still unclear.

The ESR spectrum observed in the spin-modulated phase ($\mu_0 H > H_c$) has two branches. One of them can be interpreted as uniform transversal oscillation of the magnetic moment in the field, whereas we can only speculate concerning the nature of the low frequency branch marked in Figs. 1 and 2 by "V." The frequency of the branch "V" is roughly described by expression $\nu = (g\mu_B/h)(H - H_c^*)$ with $g = 2.08$ for $H \parallel \mathbf{c}$ and $g = 2.46$ for $H \parallel \mathbf{a},\mathbf{b}$ orientations (dotted lines on Figs. 1 and 2). The value of $H_c^*$ is close to the field of transition from spiral to spin-modulated phase $H_c$. This branch was observed for magneto-ordered phase. At higher temperatures within spin-liquid phase this resonance was not detectable.

The absence of significant anisotropy allows one to suggest that this branch corresponds to an optical mode of the spin-modulated structure. The magnetic excitations of the spin-density wave phase in quasi-one-dimensional $J_N - J_{NN}$ spin systems were recently studied theoretically in Ref. [3].

The next part of the paper will describe the possible interpretation of observed absorption lines based on this theoretical model.

According to this work the gapless excitations correspond to oscillations of longitudinal components of spins. The linear with wave vector $k$ branches of these excitations have zero energy at $k = 0$ and at the wave vector of spin density wave structure $k = (\pi/2b)(1 \pm M/M_{\text{sat}})$ (see Fig. 1 from Ref. [3]) and are named as phasons. The wave vector of gapless excitations is determined by the momentum of a $Cu^{2+}$ ion $M$ normalized on their saturated value: $M_{\text{sat}} = g\mu_B S$. The phason branches of the spectra are expected to be gapless within field range of spin-density wave phase if there is no pinning of magnetic structure by crystal lattice or defects. The oscillations of perpendicular to field spin components in the two-dimensional (2D) model of weakly coupled frustrated chains [3] have gapped excitation spectrum. These branches are referred to as soliton and antisoliton. These excitations reach the lowest energy at $k = \pi/2b$ and $k = \pm(\pi/2b)M/M_{\text{sat}}$. We associate the excitations of soliton-antisoliton branches at wave vector $k = 0$ with the quasiparamagnetic branch III corresponding to the uniform oscillation of magnetic moment (see Figs. 1 and 2). Except for the branches listed, the discussed model predicts the bound states of soliton and antisoliton excitations which are referred to as breathers. The breathers of minimum energy are expected at $k = (\pi/2b)(1 \pm M/M_{\text{sat}})$ [3]. The wave vector of photons is close to zero. We expect that the resonance excitation of solitons, antisolitons, and phasons with wave vector $k \approx 0$ is possible with the ESR technique. The breather excitations near zero wave vectors have high energy.

The absolute value of wave vectors of excitations with lowest energy of solitons and antisolitons increases with field and as a result the energies of excitations at zero wave vector increase linearly with field. In the model of Ref. [3] the absolute values of wave vectors of solitons and antisolitons with minimum energy have the same wave vectors. In this case we can expect the single ESR absorption line corresponding to excitation of both solitons and antisolitons with zero wave vectors. The two branches with linear field dependence (III and V) observed in our experiments indicate lifting of degeneracy of the soliton and the antisolton excitations with $k = 0$ in $LiCuVO_4$. For an explanation of the observed ESR branches we suppose that for one branch the wave vector with minimum energy is close to theoretical [3], $k = (\pi/2b)(1 + M/M_{\text{sat}})$, and the second branch wave vector must be $k \approx (\pi/2b)(1 + M/M_{\text{sat}}) - k_{ic}$. Here $k_{ic} = 0.235 \times 4\pi/b$ is an incommensurate vector of spiral structure realized in $LiCuVO_4$ at $H < H_c$ [8]. The mechanism that can provide the splitting of soliton and antisoliton branches in the spin-modulated phase is unclear. The similar splitting of excitations of transversal components of spins was observed in a quasi-two-dimensional $S = 1/2$ antiferromagnet on triangular lattice $Cs_2CuCl_4$ and $S = 1/2$ chain antiferromagnet $K_2CuSO_4Br_2$. Here the nonequivalent behavior of spinon excitations with opposite wave vectors was observed in spin-liquid and in magneto-ordered state and was successively explained by the presence in this material of a uniform Dzyaloshinskii-Moria interaction [25–27].

The other way for interpretation of the branch "V" is associated with soliton or antisoliton excitations with frequencies at which the density of excitations is maximal, i.e., near the extremum: $k \approx \pm(\pi/2b)M/M_{\text{sat}}$.

A special mechanism is necessary for efficient excitation of such modes. There are known examples of $S = 1/2$ chain antiferromagnets, in which the magnetic excitation with large wave vectors (namely, $\pi/2$, $\pi$) were efficiently excited with radio frequency field in spin-liquid phase [28,29]. In these materials the crystallographic cell contains more than one magnetic ion. This circumstance provides the possibility to satisfy the conservation of quasimomentum. The spin structure of $LiCuVO_4$ with two copper ions in primitive cell does not allow the coupling of radio frequency field with $k \neq 0$ excitations.

Probably, the nonmagnetic defects specific for $LiCuVO_4$ provide sufficiently high efficiency of this excitation process. The excitation efficiency of standing waves is strongest when wave vectors of excitations are comparable with the characteristic distance between defects. Taking the number of defects as 0.01 of the number of magnetic ions we can expect that solitons and antisolitons possessing a suitable module of the wave vectors will be excited more efficiently. Thus, it is possible to assume that the branch "V" observed in the field range of the spin-modulated phase can be ascribed to the soliton-antisoliton excitations at wave vector close to $k = \pm(\pi/2b)M/M_{\text{sat}}$. The

energy of such excitations according to Ref. [3] grows with field increase in agreement with experiment, but the reason for the lineal increase of this energy with slope close to the slope of the paramagnetic branch $g\mu_B/h$ seems to be accidental. Thus the nature of the absorption line "V" in the spin-modulated phase is not clear. We think that this branch can be associated with excitations of soliton and antisoliton branches at $k = 0$ or $k = \pm(\pi/2b)M/M_{\rm sat}$.

Finally we would like to note that the ESR spectrum observed in the experiment in the spin-modulated phase is very similar to the spectrum computed in Ref. [30] for a 2D antiferromagnet on triangular lattice in the field range, where collinear up-up-down magnetic phase is realized. In this phase all spins are collinear to applied field as in the case discussed in the present work.

## IV. SUMMARY

We report on the ESR study of $LiCuVO_4$ in spiral and spin-modulated phases ($0 < \mu_0 H < 10$ T). The measurements have been made on high quality samples that allowed getting rid of absorption lines arising from defects. In the field range of spiral phase ($0 < \mu_0 H < 7.5$ T) all branches of the spectrum can be satisfactorily ascribed to uniform oscillations of planar spin structure. The ESR spectrum observed in spin-modulated phase ($\mu_0 H > 7.5$ T) has two branches. One of them can be explained by uniform oscillations of spin structure, whereas the second branch surprisingly demonstrates only a weak dependence on field orientation, which indicates the exchange nature of this mode. Allegedly this mode can be associated with soliton excitations. For an explanation of the effective excitation of nonuniform modes we suggest taking into consideration the nonmagnetic defects inherent to studied samples of $LiCuVO_4$.

## ACKNOWLEDGMENTS

The authors thank V. N. Glazkov, A. I. Smirnov, S. S. Sosin, and O. A. Starykh for stimulating discussions. This work is supported by the Grants of the Russian Fund for Basic Research (Grant No. 16-02-00688) and the Program of Russian Scientific Schools.

[1] T. Hikihara, L. Kecke, T. Momoi, and A. Furusaki, Phys. Rev. B **78**, 144404 (2008).
[2] S. Nishimoto, S.-L. Drechsler, R. Kuzian, J. Richter, J. Málek, M. Schmitt, J. van den Brink, and H. Rosner, Europhys. Lett. **98**, 37007 (2012).
[3] O. A. Starykh and L. Balents, Phys. Rev. B **89**, 104407 (2014).
[4] L. Kecke, T. Momoi, and A. Furusaki, Phys. Rev. B **76**, 060407(R) (2007).
[5] J. Sudan, A. Lüscher, and A. M. Läuchli, Phys. Rev. B **80**, 140402(R) (2009).
[6] M. Sato, T. Momoi, and A. Furusaki, Phys. Rev. B **79**, 060406(R) (2009).
[7] M. E. Zhitomirsky and H. Tsunetsugu, Europhys. Lett. **92**, 37001 (2010).
[8] B. J. Gibson, R. K. Kremer, A. V. Prokofiev, W. Aßmus, and G. J. McIntyre, Physica B **350**, E253 (2004).
[9] M. Enderle, C. Mukherjee, B. Fåk, R. K. Kremer, J.-M. Broto, H. Rosner, S.-L. Drechsler, J. Richter, J. Málek, A. Prokofiev, W. Aßmus, S. Pujol, J.-L. Raggazzoni, H. Rakoto, M. Rheinstädter, and H. M. Rønnow, Europhys. Lett. **70**, 237 (2005).
[10] N. Büttgen, H.-A. Krug von Nidda, L. E. Svistov, L. A. Prozorova, A. Prokofiev, and W. Aßmus, Phys. Rev. B **76**, 014440 (2007).
[11] M. Mourigal, M. Enderle, B. Fåk, R. K. Kremer, J. M. Law, A. Schneidewind, A. Hiess, and A. Prokofiev, Phys. Rev. Lett. **109**, 027203 (2012).
[12] F. Heidrich-Meisner, I. P. McCulloch, and A. K. Kolezhuk, Phys. Rev. B **80**, 144417 (2009).
[13] A. V. Chubukov, Phys. Rev. B **44**, 4693 (1991).
[14] L. E. Svistov, T. Fujita, H. Yamaguchi, S. Kimura, K. Omura, A. Prokofiev, A. I. Smirnov, Z. Honda, and M. Hagiwara, JETP Lett. **93**, 21 (2011).
[15] N. Büttgen, K. Nawa, T. Fujita, M. Hagiwara, P. Kuhns, A. Prokofiev, A. P. Reyes, L. E. Svistov, K. Yoshimura, and M. Takigawa, Phys. Rev. B **90**, 134401 (2014).
[16] A. V. Prokofiev, I. G. Vasilyeva, and V. N. Ikorskii, J. Solid State Chem. **177**, 3131 (2004).
[17] L. A. Prozorova, S. S. Sosin, L. E. Svistov, N. Büttgen, J. B. Kemper, A. P. Reyes, S. Riggs, A. Prokofiev, and O. A. Petrenko, Phys. Rev. B **91**, 174410 (2015).
[18] T. Fujita, M. Hagiwara, H. Yamaguchi, S. Kimura, L. E. Svistov, A. I. Smirnov, and A. Prokofiev, J. Phys. Soc. Jpn. **81**, SB029 (2012).
[19] A. F. Andreev and V. I. Marchenko, Usp. Fiz. Nauk **130**, 39 (1980) [Sov. Phys. Usp. **23**, 21 (1980)].
[20] H.-A. Krug von Nidda, L. E. Svistov, M. V. Eremin, R. M. Eremina, A. Loidl, V. Kataev, A. Validov, A. Prokofiev, and W. Aßmus, Phys. Rev. B **65**, 134445 (2002).
[21] P. E. Tannenwald and R. Weber, Phys. Rev. **121**, 715 (1961).
[22] H. A. Krug von Nidda, L. E. Svistov, and L. A. Prozorova, Low Temp. Phys. **36**, 736 (2010).
[23] N. Büttgen, W. Kraetschmer, L. E. Svistov, L. A. Prozorova, and A. Prokofiev, Phys. Rev. B **81**, 052403 (2010).
[24] F. C. Zhang and T. M. Rice, Phys. Rev. B **37**, 3759 (1988).
[25] K. Yu. Povarov, A. I. Smirnov, O. A. Starykh, S. V. Petrov, and A. Ya. Shapiro, Phys. Rev. Lett. **107**, 037204 (2011).
[26] A. I. Smirnov, K. Yu. Povarov, S. V. Petrov, and A. Ya. Shapiro, Phys. Rev. B **85**, 184423 (2012).
[27] A. I. Smirnov, T. A. Soldatov, K. Yu. Povarov, M. Halg, W. E. A. Lorenz, and A. Zheludev, Phys. Rev. B **92**, 134417 (2015).
[28] S. Kimura, H. Yashiro, K. Okunishi, M. Hagiwara, Z. He, K. Kindo, T. Taniyama, and M. Itoh, Phys. Rev. Lett. **99**, 087602 (2007).
[29] A. C. Tiegel, A. Honecker, T. Pruschke, A. Ponomaryov, S. A. Zvyagin, R. Feyerherm, and S. R. Manmana, Phys. Rev. B **93**, 104411 (2016).
[30] A. V. Chubukov and D. I. Golosov, J. Phys.: Condens. Matter **3**, 69 (1991).